

# Experimental Confocal Imaging for Breast Cancer Detection Using Bow-tie Antenna Array

#S. Kubota<sup>1</sup>, X. Xiao<sup>2</sup>, N. Sasaki<sup>1</sup>, A. Toya<sup>1</sup>, T. Kozaki<sup>1</sup>, M. Hanada<sup>1</sup>, T. Kikkawa<sup>1</sup>

<sup>1</sup>Research Institute for Nanodevice and Bio Systems, Hiroshima University, 1-4-2 Kagamiyama, Higashi-hiroshima, Hiroshima 739-8527, Japan, email: shinichi-kubota@hiroshima-u.ac.jp

<sup>2</sup>School of Electronic and Information Engineering, Tianjin University, Weijin Road 92, Tianjin 300072, P. R. China

## 1. Introduction

Ultra wideband (UWB) is a carrierless short range communications technology which transmits the information in the form of very short pulses.[1] The applications for short range wireless communication and microwave medical imaging [2] such as breast cancer detection are becoming more and more important. The breast cancer detection has been developed on the basis of the contrast in the electrical properties of the malignant tumor related to the normal fatty breast tissue. [3] The aim of this work is to investigate confocal imaging [4] using UWB bow-tie antenna. In this paper, experimental confocal imaging was demonstrated by averaging received waveforms as a reference waveform.

## 2. Antenna Design and Experiment

Figure 1 and shows a structure of a bow-tie antenna fabricated on a FR-4 printed circuit board (PCB) whose permittivity and  $\tan\delta$  were 3.8 and 0.0116 at 1 GHz, respectively. The antenna length of bow-tie antenna was 20 mm. The total size was 30x30 mm<sup>2</sup>. Figure 2 shows a cross-sectional view of the antenna placed on a dielectric substrate, whose permittivity and  $\tan\delta$  were 7.3 and 0.016 at 1 GHz, respectively. The antenna was connected to the pad through differential vias. The pitch and diameter of the via were 0.9 and 0.3 mm, respectively. Figure 3 shows the effect of flare angle ( $\theta$ ) of bow-tie antenna on reflection coefficient ( $S_{11}$ ). The bow-tie antenna had ultra-wideband characteristics by choosing 90°. Figure 4 shows the measurement setup for confocal imaging using Gaussian monocycle pulse (GMP). It consists of Agilent 81142A serial pulse data generator, Picosecond impulse forming networks (model 5210-104), Agilent 86100C sampling oscilloscope and a microwave probe station. Gaussian pulses from the generator were differentiated to form GMP trains by use of an impulse forming network. The measurement set-up for scattering parameters of antennas is composed of a vector network analyzer HP8510C, 180° hybrid couplers (1-12.4 GHz), SS probes and a microwave probe station [5]. Figure 5 shows the fast Fourier transformation of GMP. The center frequency and bandwidth were 6.4 and 9.8 GHz, respectively. Four fabricated antennas were aligned on a dielectric substrate [2][4]. A GMP was transmitted by one of the antennas and the reflected signals from a target were received by the rest of antennas. The measurement combination of GMP transmission was repeated. Then, the antenna array was shifted to 5, 10, 15, 20, 25 mm and measured.

## 3. Result and Discussion

Figure 6 shows the reflection coefficient ( $S_{11}$ ) of the bow-tie antenna. The bandwidth was 9.6 GHz. Figure 7 shows the transmission coefficient ( $S_{21}$ ) of the bow-tie antenna versus frequency as a parameter of transmission distance. The  $S_{21}$  at  $d = 30, 60$  and  $90$  mm were  $-17.0, -20.8$  and  $-23.1$  dB at 6 GHz, respectively. Figure 8 shows the radiation pattern at 6 GHz. The electromagnetic wave was radiated to the dielectric substrate whose dielectric constant was 7.3 by 3-dB beamwidth of 46°. Confocal imaging was performed by use of eq. (1) and (2).

$$I(r_p) = \sum_{k=1}^K \sum_{(m,n)} w(r_p) \int_0^{\tau(r_p)} (A_{m,n,k}(t) - A_{Average,m,n}(t)) dt. \quad (1)$$

$$\tau(r_p) = \left( |r_p - r_m| + |r_p - r_n| \sqrt{\epsilon_{r,substrate}} \right) / c. \quad (2)$$

The intensity of pixel  $I(r_p)$  at the position  $r_p$  in the confocal image.  $m$  and  $n$  are the indices of transmitting and receiving antennas, respectively.  $k$  and  $K$  are the index and amount of the pattern of antenna array position, respectively.  $A_{m,n,k}(t)$  means the amplitude of waveform transmitting by antenna # $m$  and receiving by antenna # $n$  at the antenna array position of # $k$ .  $\tau(r_p)$  is the propagation delay for the path  $r_m-r_p-r_n$ , where  $r_m$  and  $r_n$  are the positions of the transmitting and receiving antennas, respectively.  $\epsilon_{r,substrate}$  is the permittivity of the dielectric substrate.  $c$  is the speed of light.  $w(r_p)$  is the compensation factor for attenuation of propagation [2][4]. The reference waveform was made by averaged waveforms using eq.(3), (4) and (5)

$$A_{Average,m,n}(t) = (1/6K) \sum_{k=1}^K \sum_{(i,j) \in P} A_{i,j,k}(t), \text{ where } (m,n) = P, P = \{(1,2), (2,1), (2,3), (3,2), (3,4), (4,3)\} \quad (3)$$

$$A_{Average,m,n}(t) = (1/4K) \sum_{k=1}^K \sum_{(i,j) \in Q} A_{i,j,k}(t), \text{ where } (m,n) = Q, Q = \{(1,3), (2,4), (3,1), (4,2)\} \quad (4)$$

$$A_{Average,m,n}(t) = (1/2K) \sum_{k=1}^K \sum_{(i,j) \in R} A_{i,j,k}(t), \text{ where } (m,n) = R, R = \{(4,1), (1,4)\} \quad (5)$$

The averaged waveforms were used as a reference waveform in imaging. Figure 9 shows received waveforms and signal processing procedure. (a) As received. (b) Averaged for a reference. (c) Subtracted. (d) Integrated. (e) Compensated. The reflected waves from the target were extracted.

Figure 10(a), 10(b), 10(c) show confocal image for a dielectric target and the effect of the pitch of antenna array on image resolution. The permittivity and conductivity of dielectric target were 42.4 and 8.4 S/m at 6 GHz, respectively. The target was detected when the pitch of antenna array was smaller than 10 mm. The image of target became clear by decreasing the pitch. The dielectric target whose size was  $6 \times 6 \text{ mm}^2$  was detected.

## 4. Conclusion

The bow-tie antenna array was fabricated on a FR-4 PCB for the center frequency 6 GHz. A dielectric target whose size was  $6 \times 6 \text{ mm}^2$  and dielectric constant was 42.4 could be detected by confocal imaging of received GMP obtained with 5 mm antenna pitch and a reference waveform which were formed by averaging all received waveforms.

## Acknowledgments

This work is supported by Support Center for Advanced Telecommunications Technology Research Foundation (SCAT).

## References

- [1] T. Kikkawa, P. K. Saha, N. Sasaki, and K. Kimoto, "Gaussian Monocycle Pulse Transmitter Using 0.18  $\mu\text{m}$  CMOS Technology With On-Chip Integrated Antennas for Inter-Chip UWB Communication," IEEE Journal of Solid-State Circuits, Vol. 43, No. 5, pp.1303-1312, 2008.
- [2] E. C. Fear, X. Li, S. C. Hagness, and M. A. Stuchly, "Confocal Microwave Imaging for Breast Cancer Detection: Localization of Tumors in Three Dimensions," IEEE Trans. on Biomedical Engineering, Vol. 49, No. 8, pp. 812-822, 2002.
- [3] X. Li, and S. C. Hagness, "A Confocal Microwave Imaging Algorithm for Breast Cancer Detection," IEEE Microwave and Wireless Components Letters, Vol. 11, No. 3, pp. 130-132, 2001.
- [4] X. Xiao, and T. Kikkawa, "Early Breast Cancer Detection by Ultrawide Band Imaging with Dispersion Consideration," Japanese Journal of Applied Physics, Vol. 47, No. 4, pp. 3209-3213, 2008.
- [5] S. Kubota, X. Xiao, N. Sasaki, K. Kimoto, W. Moriyama and T. Kikkawa, "Experimental Confocal Imaging for Breast Cancer Detection Using Silicon On-Chip UWB Microantenna Array," Proc. of 2008 IEEE International Symposium on Antennas and Propagation and USNC/URSI National Radio Science Meeting, San Diego, USA, 412.1, 2008.

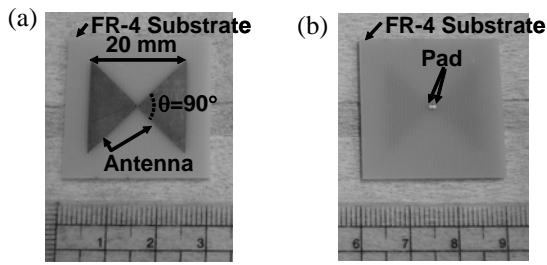


Fig. 1 Photographs of an antenna. (a) Top view. (b) Bottom view.

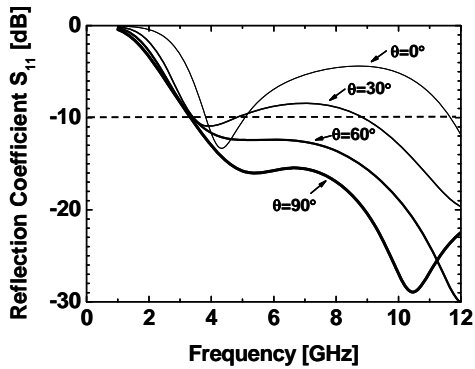


Fig. 3 The effect of flare angle of bow-tie antenna on reflection coefficient ( $S_{11}$ ).

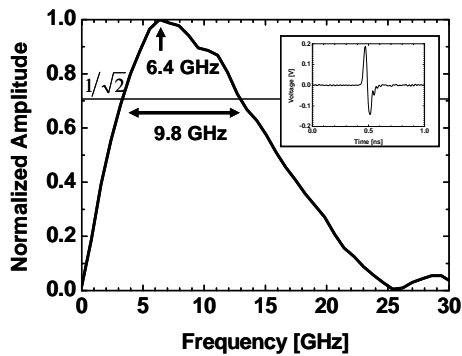


Fig. 5 Input Gaussian monocycle pulse waveform.

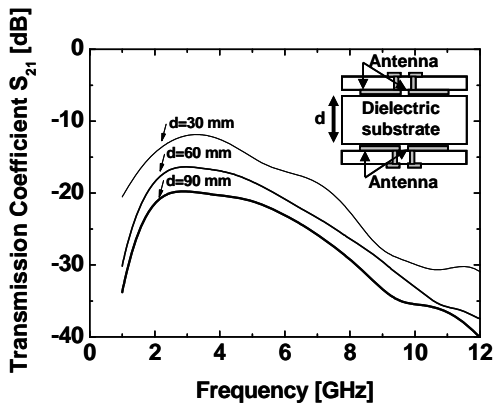


Fig. 7 Transmission Coefficient ( $S_{21}$ ) of the bow-tie antenna as a parameter of distance.

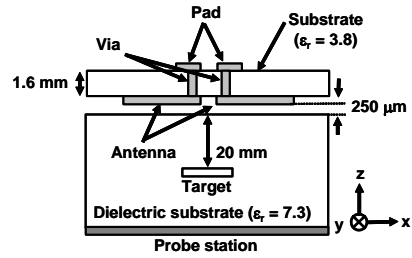


Fig. 2 Cross-sectional view of a bow-tie antenna structure and a dielectric substrate.

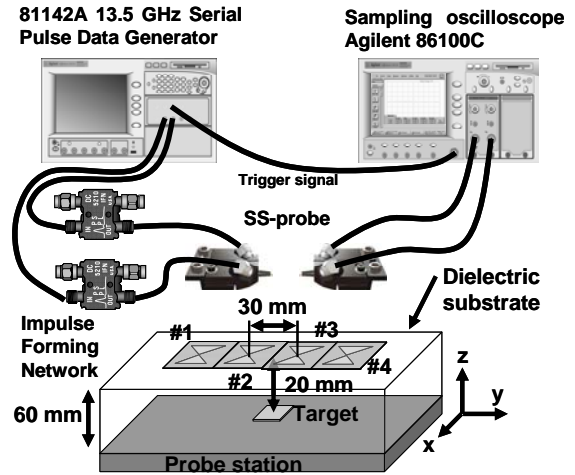


Fig. 4 Measurement setup for imaging.

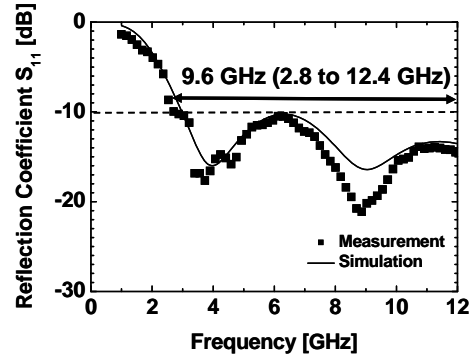


Fig. 6 Reflection coefficient ( $S_{11}$ ) of the bow-tie antenna.

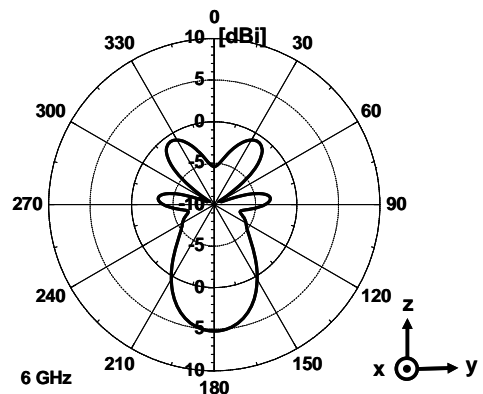


Fig. 8 Radiation pattern in y-z plane.

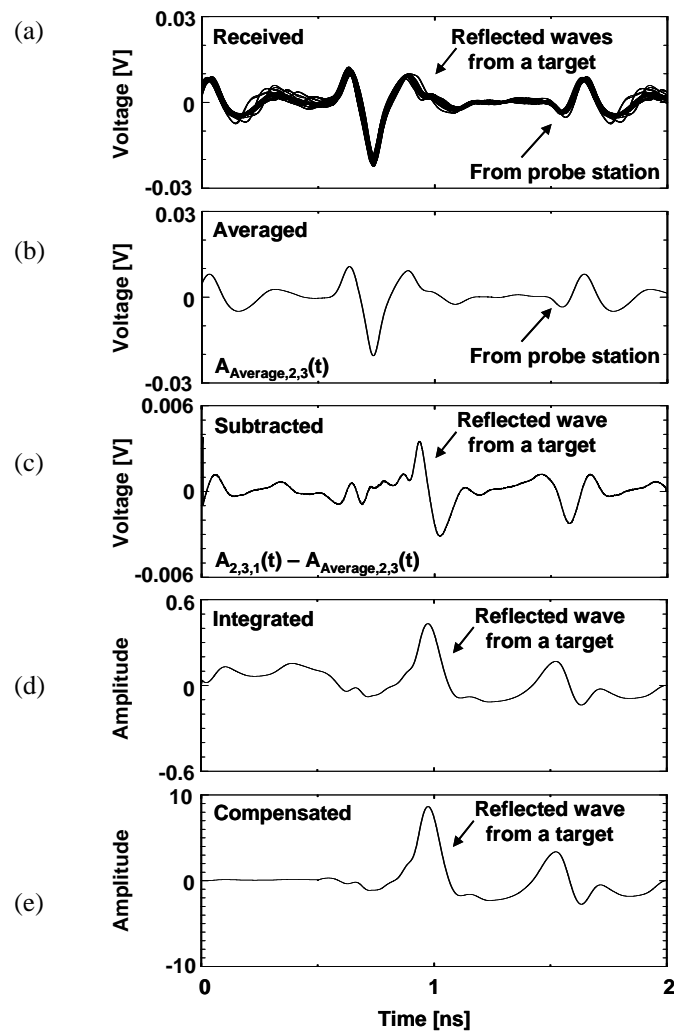


Fig. 9 Received GMP waveforms and signal processing procedure in the case that the dielectric target was  $6 \times 6 \text{ mm}^2$ . (a) As received. (b) Averaged for a reference. (c) Subtracted. (d) Integrated. (e) Compensated.

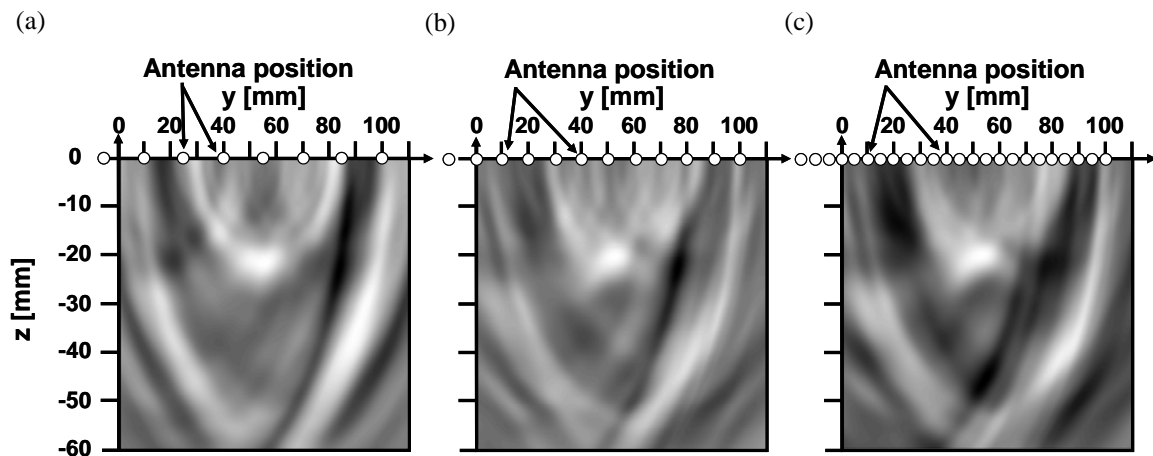


Fig. 10 Confocal imaging for a dielectric target ( $6 \times 6 \text{ mm}^2$ ). (a) Antenna pitch = 15 mm. (b) Antenna pitch = 10 mm. (c) Antenna pitch = 5 mm.